Report

Current Biology

Spectral Tuning of Phototaxis by a Go-Opsin in the Rhabdomeric Eyes of *Platynereis*

Graphical Abstract

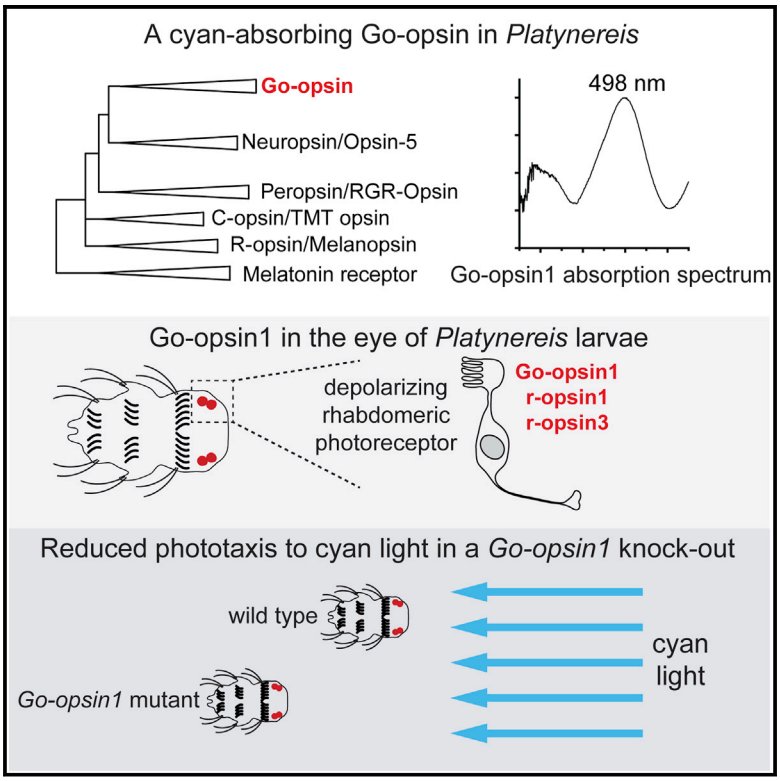

Highlights

- *Platynereis Go-opsin1* is coexpressed with r-opsins in rhabdomeric photoreceptors
- *Platynereis* Go-opsin1 forms a cyan-absorbing pigment
- A *Go-opsin1* knockout line shows reduced phototaxis efficiency to cyan light

Authors

Martin Gühmann, Huiyong Jia, Nadine Randel, ..., Nico K. Michiels, Shozo Yokoyama, Gáspár Jékely

Correspondence

gaspar.jekely@tuebingen.mpg.de

In Brief

Go-opsins represent a poorly characterized opsin family found in marine invertebrates. Gühmann et al. characterize Go-opsin1 from the marine annelid *Platynereis*. Go-opsin1 forms a cyan-absorbing pigment and is coexpressed with two r-opsins in the *Platynereis* eyes. A *Go-opsin1* knockout line shows reduced efficiency of phototaxis to cyan light.

Accession Numbers

KR869765
KR869766
KR869767
KR869768

Gühmann et al., 2015, Current Biology *25*, 2265–2271
August 31, 2015
http://dx.doi.org/10.1016/j.cub.2015.07.017

Current Biology
Report

Spectral Tuning of Phototaxis by a Go-Opsin in the Rhabdomeric Eyes of *Platynereis*

Martin Gühmann,[1] Huiyong Jia,[2] Nadine Randel,[1] Csaba Verasztó,[1] Luis A. Bezares-Calderón,[1] Nico K. Michiels,[3] Shozo Yokoyama,[2] and Gáspár Jékely[1,*]
[1]Max Planck Institute for Developmental Biology, Spemannstraße 35, 72076 Tübingen, Germany
[2]Department of Biology, Emory University, 1510 Clifton Road, Atlanta, GA 30322, USA
[3]Department of Biology, University of Tübingen, 72076 Tübingen, Germany
*Correspondence: gaspar.jekely@tuebingen.mpg.de
http://dx.doi.org/10.1016/j.cub.2015.07.017

SUMMARY

Phototaxis is characteristic of the pelagic larval stage of most bottom-dwelling marine invertebrates [1]. Larval phototaxis is mediated by simple eyes that can express various types of light-sensitive G-protein-coupled receptors known as opsins [2–8]. Since opsins diversified early during metazoan evolution in the marine environment [9], understanding underwater light detection could elucidate this diversification. Opsins have been classified into three major families, the r-opsins, the c-opsins, and the Go/RGR opsins, a family uniting Go-opsins, retinochromes, RGR opsins, and neuropsins [10, 11]. The Go-opsins form an ancient and poorly characterized group retained only in marine invertebrate genomes. Here, we characterize a Go-opsin from the marine annelid *Platynereis dumerilii* [3–5, 12–15]. We found Go-opsin1 coexpressed with two r-opsins in depolarizing rhabdomeric photoreceptor cells in the pigmented eyes of *Platynereis* larvae. We purified recombinant Go-opsin1 and found that it absorbs in the blue-cyan range of the light spectrum. To characterize the function of Go-opsin1, we generated a *Go-opsin1* knockout *Platynereis* line by zinc-finger-nuclease-mediated genome engineering. *Go-opsin1* knockout larvae were phototactic but showed reduced efficiency of phototaxis to wavelengths matching the in vitro Go-opsin1 spectrum. Our results highlight spectral tuning of phototaxis as a potential mechanism contributing to opsin diversity.

RESULTS AND DISCUSSION

Identification of Two Go-Opsins in *Platynereis*

Phylogenetic analyses indicate that three opsin families, the rhabdomeric opsins (r-opsins), the ciliary opsins (c-opsins), and the Go/RGR opsins, existed in the last common ancestor of protostomes and deuterostomes [10, 11]. These families may have diversified even earlier, before the split of cnidarians, ctenophores, and bilaterians [16]. While r-opsins and c-opsins represent visual opsins from invertebrates and vertebrates, respectively, and thus have been studied extensively, less is known about members of the Go/RGR opsin family. Among the Go/RGR opsins, RGR opsins are found in deuterostomes, lophotrochozoans, and members of the ecdysozoa. Go-opsins only exist in lophotrochozoans and non-vertebrate deuterostomes and were lost from ecdysozoans [17] and vertebrates [10].

Searching the transcriptome and genome of *Platynereis*, we found two Go-opsin-like sequences. We ran a phylogenetic analysis of these and other *Platynereis* opsins together with a representative set of metazoan opsins. The Go-opsin-like sequences grouped with lophotrochozoan and cephalochordate Go-opsins with good support in both maximum-likelihood and Bayesian analyses (Figures 1A and S1 and the Supplemental Experimental Procedures), thus establishing them as Go-opsin orthologs (called *Platynereis Go-opsin1* and *Go-opsin2*). The Go-opsins formed a well-supported clade with the RGR opsins and neuropsins/opsin5, with the neuropsins forming the sister group of the Go-opsins.

We also analyzed Go-opsins for the presence of a tripeptide motif critical for G protein binding in opsins (Figure 1B). This motif follows the transmembrane helix VII and is highly conserved in c-opsins (N[K|N]Q) and r-opsins (HP[K|R]) [12]. In contrast, we did not see a similar conservation in Go-opsins. The Go-opsin motif was more similar to c-opsins in some sequences (NNQ, *Lottia gigantea* Go-opsin1) and to r-opsins in other sequences (HKK, *Lottia gigantea* Go-opsin2). *Platynereis* Go-opsin1 and Go-opsin2 had intermediate versions of the motifs (NRK and NKK, respectively). This suggests that during evolution, Go-opsins may switch the subtype of G protein to which they couple.

Go-opsin1 Coexpresses with Two r-Opsins in the Rhabdomeric Adult Eyes of *Platynereis*

The first Go-opsin was identified in the scallop mantle-edge eye [18]. The scallop retina has one layer of rhabdomeric and one layer of ciliary photoreceptor cells [19]. The Go-opsin is only expressed in the ciliary photoreceptor cell layer [18]. *Platynereis* larvae also have both ciliary and rhabdomeric photoreceptor cells. The ciliary photoreceptor cells found in the larval brain are not associated with shading pigment [12]. In contrast, the rhabdomeric photoreceptor cells are associated with pigment cells and are found in the eyespots (ocelli or larval eyes) and in two pairs of simple pigment-cup eyes (adult eyes) (Figures 2A–2C) [3, 4]. We characterized the expression of

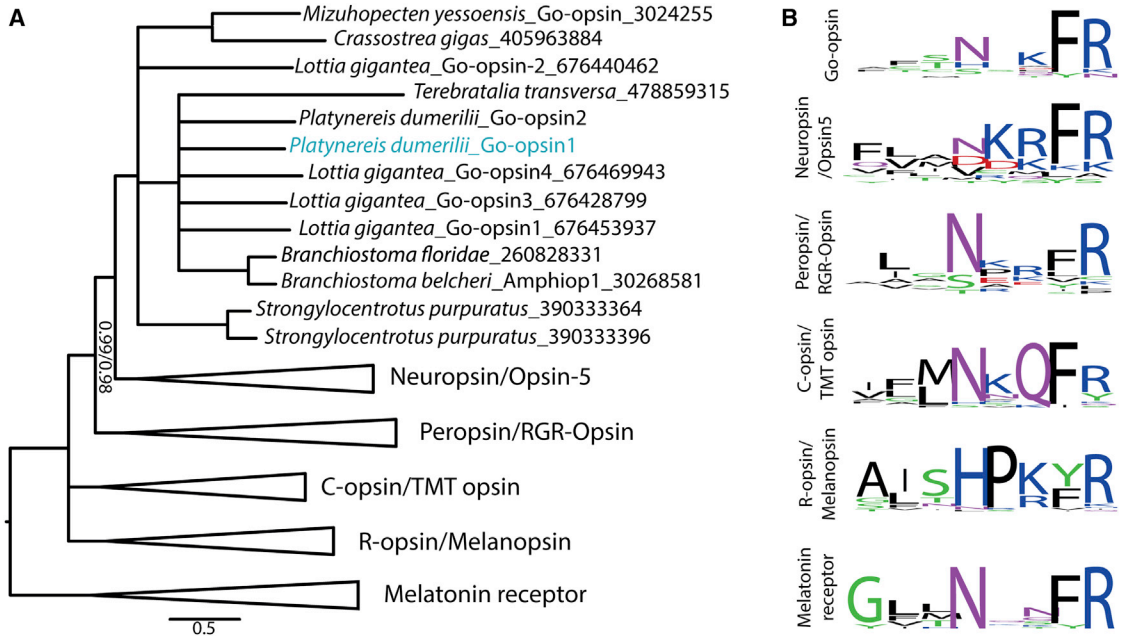

Figure 1. Phylogeny of *Platynereis* Go-Opsins

(A) Phylogenetic tree showing *Platynereis* Go-opsin1 and Go-opsin2 grouped with other Go-opsins. All nodes had support values >0.99 in both maximum-likelihood and Bayesian trees, unless otherwise indicated. Groups that were not supported in both trees to >0.9 were brought back to the next well-supported node.

(B) Sequence logos of a sequence stretch immediately after helix VII are shown for each opsin group.

Go-opsin1 in 3-day-old *Platynereis* larvae by double whole-mount in situ hybridization with a probe for *Go-opsin1* and a probe for the rhabdomeric-photoreceptor-cell-specific opsin, *r-opsin1* [5]. The *Go-opsin1*-specific probe labeled the eyespots and the adult eyes, as well as one cell of unknown nature in the dorsal median head close to the ciliary photoreceptor cells (Figure 2D, arrowhead), but did not label the ciliary photoreceptor cells (Figure 2D). In the eyespots and the adult eyes, *Go-opsin1* and *r-opsin1* were coexpressed in the same rhabdomeric photoreceptor cells (Figures 2D–2H). In the *Platynereis* adult eyes, *r-opsin1* is also known to be coexpressed with *r-opsin3* [8], indicating that the photoreceptor cells of the adult eyes coexpress all three opsins. As we were unable to detect expression of *Go-opsin2* by in situ hybridization in the larvae, we focused on *Go-opsin1* for further characterization.

The coexpression of *Go-opsin1* with two r-opsins in rhabdomeric photoreceptor cells was unexpected, given that a Go-opsin is expressed in ciliary photoreceptor cells in the scallop eye and that opsins belonging to two different families generally do not coexpress in the same cell. One exception is the coexpression of a rhabdomeric opsin and a retinochrome, a photoisomerase also belonging to the Go/RGR opsin family, in cephalopod and gastropod photoreceptor cells [20–22].

Spectral Characterization of *Platynereis* Go-opsin1

To characterize the spectral sensitivity of the opsins expressed in the *Platynereis* eyes, we tried to purify recombinant proteins. In general, it has proven extremely difficult to reconstruct invertebrate photopigments in vitro [23]. We could not obtain structurally stable r-opsin pigments; however, we could purify stable Go-opsin1 from COS1 cells and reconstituted it with 11-*cis*-retinal [24]. The Go-opsin1 pigment absorbed in the cyan range of the spectrum, with a λ_{max} of 488 nm in the dark spectrum (Figure 3A). When the pigment was exposed to light for 30 min, the absorption peak at 488 nm was reduced. The dark-light difference spectrum (calculated by subtraction of the post-illumination spectrum from the pre-illumination spectrum) gave a λ_{max} of 498 nm (Figure 3A, inset, and Table S1). In vitro analysis of a Go-opsin from the amphioxus *Branchiostoma belcheri* found a similar spectral sensitivity with a λ_{max} of 483 nm [25, 26].

Platynereis Rhabdomeric Photoreceptor Cells Depolarize at Both Violet and Cyan Stimulation

In the scallop retina, the rhabdomeric photoreceptor cells are depolarizing and the ciliary photoreceptor cells are hyperpolarizing [19]. This hyperpolarizing response is thought to be mediated by a Go-opsin with downstream Go-alpha signaling [18, 27]. In contrast, r-opsins generally mediate a depolarizing response. This suggests that Go-opsin1 and the r-opsins may mediate antagonistic phototransduction pathways in the *Platynereis* eye. Such an antagonism between opsins has already been described for pinopsin and parietopsin in the lizard parietal eye [28].

To test whether *Go-opsin1* mediates a hyperpolarizing response in the *Platynereis* rhabdomeric photoreceptor cells, we used calcium imaging to measure direct photoresponses from the adult eyes. We ubiquitously expressed a calcium indicator, GCaMP6s, in *Platynereis* larvae, and measured photoreceptor responses to different light wavelengths. The photoreceptor cell rhabdoms inside the pigment cup of the adult eye were

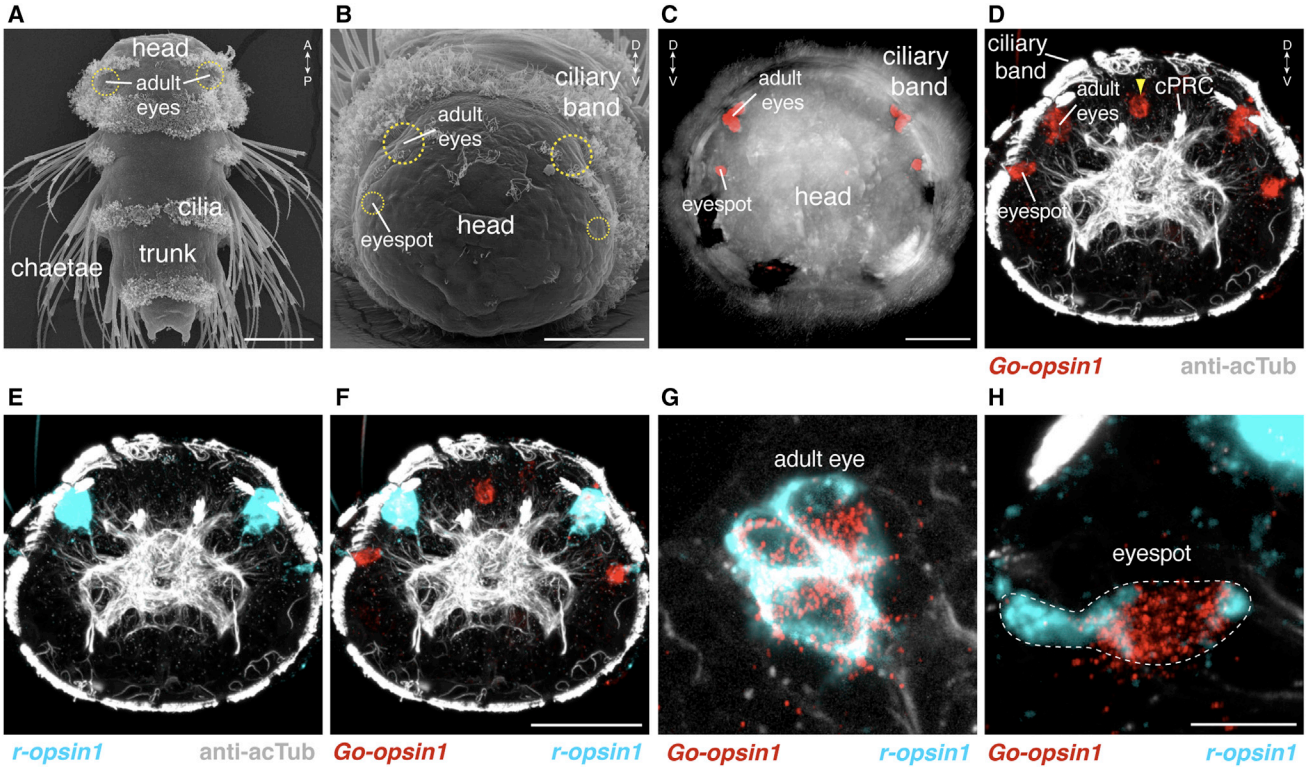

Figure 2. *Go-opsin1* Is Expressed in Rhabdomeric Photoreceptor Cells in the *Platynereis* Larva

(A and B) Scanning electron microscopy images of a 72 hr post-fertilization (hpf) *Platynereis* larvae, ventral (A) and anterior (B) views. Anterior-posterior and dorso-ventral axes are indicated.

(C) Differential interference contrast (DIC) image of a 72 hpf *Platynereis* larva with the pigment of the eyespots and adult eyes shown in red, anterior view.

(D–H) Double whole-mount mRNA in situ hybridization for *Platynereis Go-opsin1* (D) and *r-opsin1* (E) counterstained for acetylated alpha-tubulin (white) in a 72 hpf larva, anterior view. Merged images are shown in (F)–(H). The two opsins coexpress in the adult eye photoreceptor cells (G) and one photoreceptor cell of the eyespot (H).

Scale bars represent 50 μm (A), 20 μm (B), 30 μm (C), 50 μm (F), and 10 μm (H). cPRC, ciliary photoreceptor cell. See also Figure S1 and the Supplemental Experimental Procedures.

locally stimulated, and the responses were recorded from the adjacent photoreceptor cell-body region (Figures 3B–3D and the Supplemental Experimental Procedures). When the photoreceptor cells were stimulated with cyan (488 nm) laser light, matching the peak absorption of Go-opsin1, the intracellular calcium levels reproducibly increased, which indicates photoreceptor cell depolarization. This suggests that in *Platynereis*, unlike in the scallop, Go-opsin1 does not mediate hyperpolarization. We also stimulated the *Platynereis* photoreceptor cells with violet light (405 nm) and again found reproducible depolarizing responses (Figure 3D). The lack of a hyperpolarizing response to either cyan or violet light stimulation suggests that Go-opsin1 does not antagonize the r-opsins in the *Platynereis* eye.

Genetic Engineering of a *Go-opsin1* Knockout *Platynereis* Line

To analyze the function of Go-opsin1 in *Platynereis*, we generated a *Go-opsin1* knockout line. We targeted the first exon of the *Go-opsin1* locus encoding the N terminus before the first transmembrane domain. We used engineered zinc-finger nuclease (ZFN) constructs and injected ZFN mRNA into fertilized eggs. The injected individuals were raised to adulthood and crossed to wild-type animals, and a subset of their progeny was screened for inherited genomic lesions. We screened 51 batches of larvae and found one batch that carried an 8-bp deletion, leading to a frame-shift and a premature STOP codon in the *Go-opsin1* coding region (Figures 4A and 4B). This most likely represents a *Go-opsin1* null allele (*Go-opsin1*$^{\Delta 8}$). We crossed heterozygous carriers of the mutation and established a homozygous *Go-opsin1*$^{\Delta 8/\Delta 8}$ mutant line. Due to the low efficiency of ZFN cleavage, we were unable to isolate further *Go-opsin1* mutant alleles. The *Go-opsin1*$^{\Delta 8/\Delta 8}$ mutants were viable and fertile and displayed a normal lunar cycle of reproduction, similar to wild-type worms (Figure S2A).

Reduced Phototaxis Efficiency in *Go-opsin1*$^{\Delta 8/\Delta 8}$ Knockout Larvae

For functional analysis of Go-opsin1, we focused on the phototactic behavior displayed by 3- to 4-day-old *Platynereis* nectochaete larvae. At this stage, phototaxis is mediated exclusively by the two pairs of adult eyes, as demonstrated by eye-ablation experiments [4]. To determine the function of Go-opsin1 in the rhabdomeric photoreceptor cells of the adult eyes, we measured

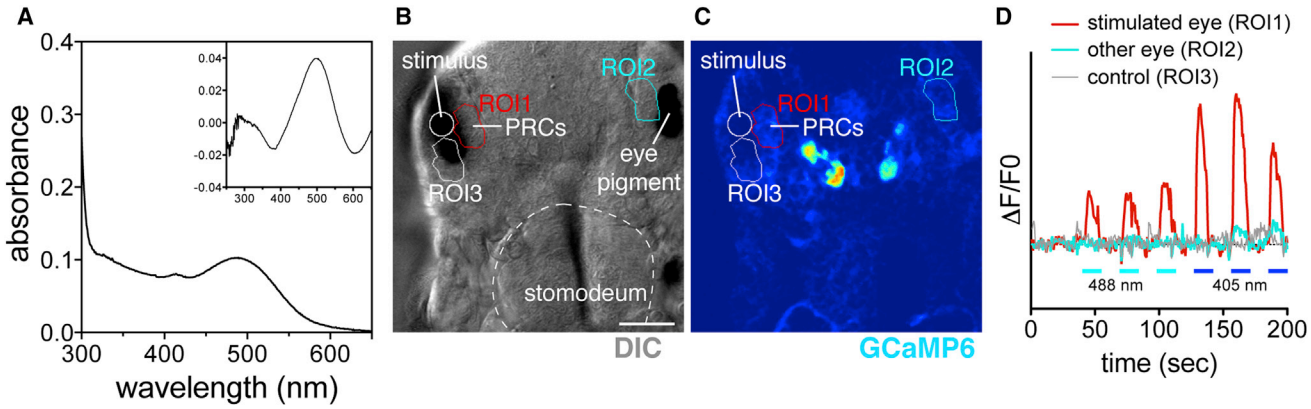

Figure 3. Absorption Spectrum of *Platynereis* Go-Opsin and Depolarizing Responses of the Photoreceptor Cells

(A) Absorption spectrum of the *Platynereis* Go-opsin1 pigment in the dark and the dark-light difference spectrum (inset).

(B) DIC image showing the position of the eyes, the local stimulation, and the regions of interest (ROIs) used to record calcium signals. The scale bar represents 20 μm.

(C) Snapshot of a calcium-imaging video showing GCaMP6 fluorescence, the region of local stimulation, and the ROIs used to record calcium signals.

(D) Calcium imaging curves showing ΔF/F0 signals upon stimulation with 488-nm and 405-nm light.

The region of the stimulation is marked in (B) and (C). PRC, photoreceptor cell. See also Table S1 and the Supplemental Experimental Procedures.

the phototaxis efficiency of wild-type larvae and *Go-opsin1*$^{\Delta 8/\Delta 8}$ mutant larvae in response to monochromatic light stimuli of different wavelengths.

3- to 4-day-old *Platynereis* larvae can display both positive and negative phototaxis and may switch the sign of phototaxis during an experiment [4]. To characterize both negative and positive phototaxis, we used two different experimental setups. In a vertical-column setup, we stimulated larvae with collimated monochromatic light from the top. In this setup, the larvae showed positive phototaxis to light in the blue-green range of the spectrum. In contrast, in a horizontal setup with a glass beaker and illumination from one side, initially photopositive larvae turned photonegative after light exposure. Therefore, in this setup, we could consistently measure negative phototaxis (Movie S1).

We found that light intensity strongly influenced the spectral range of the phototactic response. At high light intensity, we could trigger phototaxis between 340 and 680 nm, but at a lower intensity, there was no response to red or UV light (Figures S2C and S2D). However, the photon flux of our light source was not completely constant across all wavelengths, which may conflate the effects of wavelength and intensity in the action spectra. We could not measure photon fluxes below 380 nm with our spectrophotometer, but we confirm that total irradiance as experienced by the larvae was comparable between 400 and 600 nm (3.2E+18 to 4.3E+18 photons/s/m^2; Figure S2B). Therefore, we only compared wild-type and mutant larvae at different monochromatic illumination treatments in this wavelength range, without describing a full action spectrum.

Both wild-type and *Go-opsin1*$^{\Delta 8/\Delta 8}$ knockout larvae were phototactic toward light in the blue-green range of the spectrum in both setups (Figures 4C and 4D). However, the *Go-opsin1*$^{\Delta 8/\Delta 8}$ knockout larvae showed significantly reduced efficiency of phototaxis to cyan light in both setups. In the horizontal setup the knockout larvae showed significantly reduced phototaxis at 500 nm and 520 nm, and in the vertical setup at 480 nm and 500 nm. We also measured positive phototaxis of heterozygous *Go-opsin1*$^{\Delta 8/+}$ larvae and found that they showed intermediate values not significantly different from those of either wild-type or homozygous mutant larvae. This is consistent with an expected reduction in Go-opsin1 levels in heterozygous larvae. In both setups, we measured the largest difference between the means of wild-type and homozygous mutant larvae at 500 nm (Figures S2E and S2F). This agrees well with the in vitro spectrum of the Go-opsin1 photopigment, which has a λ_{max} of 488 nm in the dark spectrum and a λ_{max} of 498 nm in the dark-light spectrum (Figure 3A). Although the effect sizes were small, the in vitro spectrum of Go-opsin1 closely matched the spectral range of the behavioral defects determined in two independent behavioral assays, indicating that the defects in the mutants were due to the loss of the Go-opsin1 pigment. This suggests that Go-opsin1 contributes to phototaxis and enhances the efficiency of this behavior in the blue-cyan part of the light spectrum.

The blue-cyan range with a peak at 480 nm represents the wavelengths that penetrate seawater the deepest, as shown by our underwater field recordings from the coastal waters of Corsica in the Mediterranean (Figures S2G and S2H), an area inhabited by *Platynereis* [15]. Thus, Go-opsin1 may be spectrally tuned to enhance the sensitivity of *Platynereis* phototaxis to wavelengths of light that maximally penetrate seawater. Go-opsin1 must also work together with other photopigments to mediate phototaxis, since phototaxis persists, albeit with reduced efficiency, in the *Go-opsin1* knockout larvae. Since Go-opsin1 is coexpressed with the two r-opsins in the same photoreceptor cells, these opsins most likely also contribute to phototaxis.

Understanding the function of opsins in the marine environment is essential to our understanding of why opsins diversified into several families early during animal evolution. It has been proposed that different opsins may initially have been coexpressed in the same photoreceptor cells and diversified to

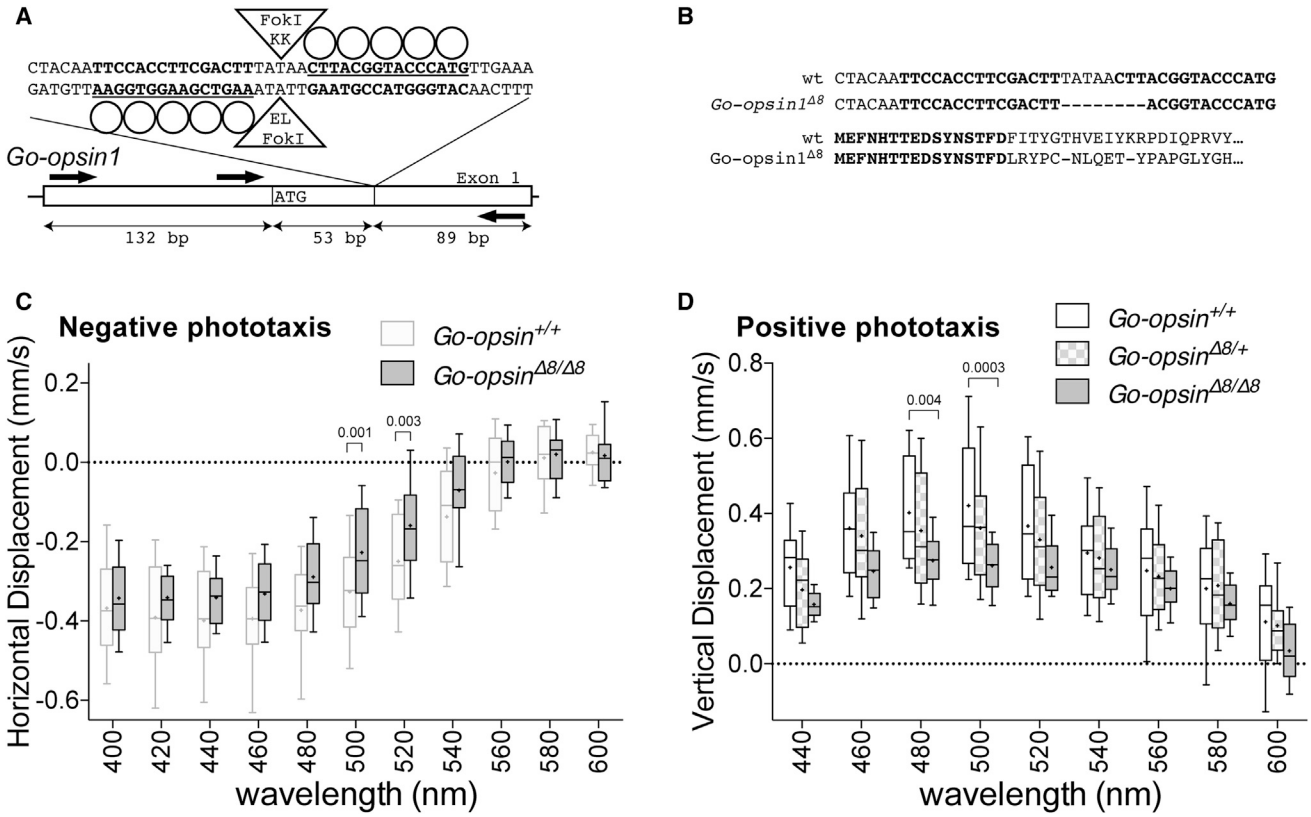

Figure 4. Reduced Efficiency of Phototaxis in *Go-opsin1*$^{\Delta 8/\Delta 8}$ Mutant Larvae

(A) Genomic region of *Go-opsin1* targeted by the ZFN. Circles indicate the base pairs recognized by the individual zinc fingers. The cleavage site of the FokI nuclease is indicated by triangles.

(B) 8-bp deletion in the *Go-opsin1*$^{\Delta 8}$ mutant allele. The mutation leads to a frame-shift and an early STOP codon in *Go-opsin1*.

(C) Efficiency of negative phototaxis of wild-type and *Go-opsin1*$^{\Delta 8/\Delta 8}$ larvae to different wavelengths of light. Whiskers in the box plot indicate 10th–90th percentile; means are indicated with a dot. n = 31 batches for wild-type and n = 25 batches for *Go-opsin1*$^{\Delta 8/\Delta 8}$ mutant larvae. Each batch contained >50 larvae.

(D) Efficiency of positive phototaxis of wild-type, *Go-opsin1*$^{\Delta 8/+}$, and *Go-opsin1*$^{\Delta 8/\Delta 8}$ larvae to different wavelengths of light. Whiskers in the box plot indicate 10th–90th percentile; means are indicated with a dot. n = 13 homozygous and heterozygous and n = 14 wild-type batches with >50 larvae each.

p values (<0.05) of unpaired t tests are shown for comparisons between wild-type mutant that were significantly different after Sidak-Bonferroni correction. See also Figure S2.

mediate antagonistic signaling pathways [9]. Alternatively, opsins may have diversified to cover different parts of the spectrum. Our work revealed how Go-opsin1 contributes to phototaxis in the rhabdomeric adult eyes of the planktonic larva of *Platynereis*. The coexpression of Go-opsin1 with the r-opsins represents another example of the coexpression and functional integration of two opsins belonging to different families. This suggests a scenario where opsins may have initially diversified within the same photoreceptor cell to cover a broader response spectrum. Further in vitro and genetic studies of Go-opsins will be needed to understand how changes in G protein coupling may have contributed to this diversification.

EXPERIMENTAL PROCEDURES

Animal Culture

Animals were obtained from an established breeding culture [29] kept at 22°C. *Platynereis* larvae were kept at 18°C in a 16 hr light/8 hr dark cycle until behavioral experiments. The experiments were conducted at room temperature. The research fully abided to the regulations of Directive 2010/63/EU of the European Parliament and of the Council on the protection of animals used for scientific purposes.

In Situ Hybridization

Whole-mount in situ hybridization and confocal imaging were done as previously described [30–32].

ZFN Design and Microinjection

Before ZFN design, splice sites and polymorphic sites in our laboratory culture were identified. A custom ZFN pair targeting the first exon of *Platynereis Go-opsin1* was designed and generated (Sigma-Aldrich). The ZFNs used the EL:KK FokI obligate heterodimer system to reduce off-target cleavage [33]. The ZFN recognition site was 5′-AAGGTGGAAGCTGAAatatt GAATGCCATGGGTAC-3′. The binding sites are given in uppercase and the cut site in lowercase. The sequence is complementary to the coding sequence.

ZFN mRNA in a concentration of 40 ng/μl was injected into fertilized eggs of *Platynereis* wild-type parents according to an established injection procedure [34]. The eggs were kept at 18°C for 45 min before injection and were injected at 14.5°C. The injected individuals were kept at 18°C for 5 to 8 days in 6-well-plates (Nunc multidish no. 150239, Thermo Scientific) and then cultured at 22°C until sexual maturity. The mature worms were crossed to wild-type

worms and the progeny was genotyped, resulting in one founder line, which was bred to homozygosity.

Calcium Imaging

Calcium imaging was carried out on 4-day-old *Platynereis* larvae that had been injected in one-cell-stage with capped and polyA-tailed GCaMP6s mRNA [35] as previously described [4]. Movies were analyzed with custom Fiji [36] and Python scripts, following [37]. See the Supplemental Experimental Procedures for details. Scripts are available at https://github.com/JekelyLab/Phototaxis.

In Vitro Opsin Assay

Recombinant Go-opsin1 was purified and analyzed following [24]. See the Supplemental Experimental Procedures for details.

Molecular Phylogeny

We found the *Platynereis* opsins *Go-opsin1*, *Go-opsin2, r-opsin2*, *r-opsin5*, and *neuropsin-2* in a transcriptome assembly generated by Trinity [38]. *Go-opsin1*, *Go-opsin2*, *r-opsin2*, and *r-opsin5* were cloned from cDNA and sequenced (GenBank: KR869765, KR869766, KR869767, and KR869768). All other Platynereis *opsins* were reported previously [8, 12, 39, 40]. We inferred the opsin phylogeny with an established pipeline [8]. For maximum-likelihood and Bayesian analysis, we used PhyML [41] and MrBayes [42], respectively. See the Supplemental Experimental Procedures for details, alignment, and sequence identifiers.

Phototaxis Assays

Phototaxis of *Platynereis* nectochaete larvae was assayed in two different experimental setups. To measure negative phototaxis, we used 100-ml glass beakers. To measure positive phototaxis, we used a vertical column (32 × 10 × 160 mm). The larvae were stimulated with monochromatic light provided by a monochromator (PolyChrome II, Till Photonics). Photon fluxes are shown in Figure S2B. Based on the field measurements (Figures S2G and S2H), we estimate that the stimulus light we used corresponds to photon fluxes that occur at a depth of approximately 40–50 m in the Mediterranean on a bright summer day at noon. The larvae in the videos were tracked with the ImageJ plugin mTRack2. The tracks were analyzed with a Perl script that extracted the average displacement of the larvae along the axis parallel to the light vector. See the Supplemental Experimental Procedures for details. Scripts are available at https://github.com/JekelyLab/Phototaxis.

Measurement of Photon Irradiance

Total photon irradiance (photons/s/m^2) was measured with a calibrated PR-670 PhotoResearch photospectrometer with a CR-670 cosine-corrected accessory to measure irradiance directly while aimed to the source. See the Supplemental Experimental Procedures for details.

ACCESSION NUMBERS

The accession numbers for the *Platynereis* opsins reported in this paper are GenBank: KR869765, KR869766, KR869767, and KR869768.

SUPPLEMENTAL INFORMATION

Supplemental Information includes Supplemental Experimental Procedures, two figures, one table, and one movie and can be found with this article online at http://dx.doi.org/10.1016/j.cub.2015.07.017.

AUTHOR CONTRIBUTIONS

M.G. generated the Go-opsin1 knockout line and conducted and analyzed the behavioral experiments. H.J. and S.Y. measured and analyzed the in vitro opsin spectrum. N.R. conducted the calcium imaging experiments. C.V. wrote the calcium-imaging analysis script. L.A.B.-C. did the phylogenetic analysis. N.K.M. measured the underwater light spectra and photon fluxes in the phototaxis setup. G.J. did the double in situ hybridization and wrote the paper, with contributions from all coauthors.

ACKNOWLEDGMENTS

We thank Elizabeth Williams for comments. The research leading to these results received funding from the European Research Council under the European Union's Seventh Framework Programme (FP7/2007-2013)/European Research Council grant agreement 260821. S.Y. was supported by the NIH (R01EY016400) and Emory University.

Received: April 11, 2015
Revised: May 26, 2015
Accepted: July 7, 2015
Published: August 6, 2015

REFERENCES

1. Thorson, G. (1964). Light as an ecological factor in the dispersal and settlement of larvae of marine bottom invertebrates. Ophelia *1*, 167–208.
2. Arendt, D., and Wittbrodt, J. (2001). Reconstructing the eyes of Urbilateria. Philos. Trans. R. Soc. Lond. B Biol. Sci. *356*, 1545–1563.
3. Jékely, G., Colombelli, J., Hausen, H., Guy, K., Stelzer, E., Nédélec, F., and Arendt, D. (2008). Mechanism of phototaxis in marine zooplankton. Nature *456*, 395–399.
4. Randel, N., Asadulina, A., Bezares-Calderón, L.A., Verasztó, C., Williams, E.A., Conzelmann, M., Shahidi, R., and Jékely, G. (2014). Neuronal connectome of a sensory-motor circuit for visual navigation. eLife *3*, e02730.
5. Arendt, D., Tessmar, K., de Campos-Baptista, M.-I.M., Dorresteijn, A., and Wittbrodt, J. (2002). Development of pigment-cup eyes in the polychaete *Platynereis dumerilii* and evolutionary conservation of larval eyes in Bilateria. Development *129*, 1143–1154.
6. Passamaneck, Y.J., Furchheim, N., Hejnol, A., Martindale, M.Q., and Lüter, C. (2011). Ciliary photoreceptors in the cerebral eyes of a protostome larva. Evodevo *2*, 6.
7. Vopalensky, P., Pergner, J., Liegertova, M., Benito-Gutierrez, E., Arendt, D., and Kozmik, Z. (2012). Molecular analysis of the amphioxus frontal eye unravels the evolutionary origin of the retina and pigment cells of the vertebrate eye. Proc. Natl. Acad. Sci. USA *109*, 15383–15388.
8. Randel, N., Bezares-Calderón, L.A., Gühmann, M., Shahidi, R., and Jékely, G. (2013). Expression dynamics and protein localization of rhabdomeric opsins in *Platynereis* larvae. Integr. Comp. Biol. *53*, 7–16.
9. Nilsson, D.-E. (2013). Eye evolution and its functional basis. Vis. Neurosci. *30*, 5–20.
10. Porter, M.L., Blasic, J.R., Bok, M.J., Cameron, E.G., Pringle, T., Cronin, T.W., and Robinson, P.R. (2012). Shedding new light on opsin evolution. Proc. Biol. Sci. *279*, 3–14.
11. Feuda, R., Hamilton, S.C., McInerney, J.O., and Pisani, D. (2012). Metazoan opsin evolution reveals a simple route to animal vision. Proc. Natl. Acad. Sci. USA *109*, 18868–18872.
12. Arendt, D., Tessmar-Raible, K., Snyman, H., Dorresteijn, A.W., and Wittbrodt, J. (2004). Ciliary photoreceptors with a vertebrate-type opsin in an invertebrate brain. Science *306*, 869–871.
13. Zantke, J., Bannister, S., Rajan, V.B.V., Raible, F., and Tessmar-Raible, K. (2014). Genetic and genomic tools for the marine annelid *Platynereis dumerilii*. Genetics *197*, 19–31.
14. Bannister, S., Antonova, O., Polo, A., Lohs, C., Hallay, N., Valinciute, A., Raible, F., and Tessmar-Raible, K. (2014). TALENs mediate efficient and heritable mutation of endogenous genes in the marine annelid *Platynereis dumerilii*. Genetics *197*, 77–89.
15. Fischer, A., and Dorresteijn, A. (2004). The polychaete *Platynereis dumerilii* (Annelida): a laboratory animal with spiralian cleavage, lifelong segment proliferation and a mixed benthic/pelagic life cycle. BioEssays *26*, 314–325.
16. Feuda, R., Rota-Stabelli, O., Oakley, T.H., and Pisani, D. (2014). The comb jelly opsins and the origins of animal phototransduction. Genome Biol. Evol. *6*, 1964–1971.

17. Hering, L., and Mayer, G. (2014). Analysis of the opsin repertoire in the tardigrade *Hypsibius dujardini* provides insights into the evolution of opsin genes in panarthropoda. Genome Biol. Evol. *6*, 2380–2391.
18. Kojima, D., Terakita, A., Ishikawa, T., Tsukahara, Y., Maeda, A., and Shichida, Y. (1997). A novel Go-mediated phototransduction cascade in scallop visual cells. J. Biol. Chem. *272*, 22979–22982.
19. McReynolds, J.S., and Gorman, A.L. (1970). Photoreceptor potentials of opposite polarity in the eye of the scallop, *Pecten irradians*. J. Gen. Physiol. *56*, 376–391.
20. Ozaki, K., Hara, R., and Hara, T. (1983). Histochemical localization of retinochrome and rhodopsin studied by fluorescence microscopy. Cell Tissue Res. *233*, 335–345.
21. Terakita, A., Hara, R., and Hara, T. (1989). Retinal-binding protein as a shuttle for retinal in the rhodopsin-retinochrome system of the squid visual cells. Vision Res. *29*, 639–652.
22. Katagiri, N., Terakita, A., Shichida, Y., and Katagiri, Y. (2001). Demonstration of a rhodopsin-retinochrome system in the stalk eye of a marine gastropod, *Onchidium*, by immunohistochemistry. J. Comp. Neurol. *433*, 380–389.
23. Knox, B.E., Salcedo, E., Mathiesz, K., Schaefer, J., Chou, W.-H., Chadwell, L.V., Smith, W.C., Britt, S.G., and Barlow, R.B. (2003). Heterologous expression of limulus rhodopsin. J. Biol. Chem. *278*, 40493–40502.
24. Yokoyama, S. (2000). Phylogenetic analysis and experimental approaches to study color vision in vertebrates. Methods Enzymol. *315*, 312–325.
25. Koyanagi, M., Terakita, A., Kubokawa, K., and Shichida, Y. (2002). Amphioxus homologs of Go-coupled rhodopsin and peropsin having 11-cis- and all-trans-retinals as their chromophores. FEBS Lett. *531*, 525–528.
26. Tsukamoto, H., Terakita, A., and Shichida, Y. (2005). A rhodopsin exhibiting binding ability to agonist all-trans-retinal. Proc. Natl. Acad. Sci. USA *102*, 6303–6308.
27. Gomez, M.P., and Nasi, E. (2000). Light transduction in invertebrate hyperpolarizing photoreceptors: possible involvement of a Go-regulated guanylate cyclase. J. Neurosci. *20*, 5254–5263.
28. Su, C.-Y., Luo, D.-G., Terakita, A., Shichida, Y., Liao, H.-W., Kazmi, M.A., Sakmar, T.P., and Yau, K.-W. (2006). Parietal-eye phototransduction components and their potential evolutionary implications. Science *311*, 1617–1621.
29. Hauenschild, C., and Fischer, A. (1969). *Platynereis dumerilii*. Mikroskopische Anatomie, Fortpflanzung, Entwicklung (Stuttgart: Gustav Fischer).
30. Tessmar-Raible, K., Steinmetz, P.R.H., Snyman, H., Hassel, M., and Arendt, D. (2005). Fluorescent two-color whole mount in situ hybridization in *Platynereis dumerilii* (Polychaeta, Annelida), an emerging marine molecular model for evolution and development. Biotechniques *39*, 460, 462, 464.
31. Jékely, G., and Arendt, D. (2007). Cellular resolution expression profiling using confocal detection of NBT/BCIP precipitate by reflection microscopy. Biotechniques *42*, 751–755.
32. Asadulina, A., Panzera, A., Verasztó, C., Liebig, C., and Jékely, G. (2012). Whole-body gene expression pattern registration in Platynereis larvae. Evodevo *3*, 27.
33. Miller, J.C., Holmes, M.C., Wang, J., Guschin, D.Y., Lee, Y.-L., Rupniewski, I., Beausejour, C.M., Waite, A.J., Wang, N.S., Kim, K.A., et al. (2007). An improved zinc-finger nuclease architecture for highly specific genome editing. Nat. Biotechnol. *25*, 778–785.
34. Conzelmann, M., Williams, E.A., Tunaru, S., Randel, N., Shahidi, R., Asadulina, A., Berger, J., Offermanns, S., and Jékely, G. (2013). Conserved MIP receptor-ligand pair regulates *Platynereis* larval settlement. Proc. Natl. Acad. Sci. USA *110*, 8224–8229.
35. Chen, T.-W., Wardill, T.J., Sun, Y., Pulver, S.R., Renninger, S.L., Baohan, A., Schreiter, E.R., Kerr, R.A., Orger, M.B., Jayaraman, V., et al. (2013). Ultrasensitive fluorescent proteins for imaging neuronal activity. Nature *499*, 295–300.
36. Schindelin, J., Arganda-Carreras, I., Frise, E., Kaynig, V., Longair, M., Pietzsch, T., Preibisch, S., Rueden, C., Saalfeld, S., Schmid, B., et al. (2012). Fiji: an open-source platform for biological-image analysis. Nat. Methods *9*, 676–682.
37. Jia, H., Rochefort, N.L., Chen, X., and Konnerth, A. (2011). In vivo two-photon imaging of sensory-evoked dendritic calcium signals in cortical neurons. Nat. Protoc. *6*, 28–35.
38. Grabherr, M.G., Haas, B.J., Yassour, M., Levin, J.Z., Thompson, D.A., Amit, I., Adiconis, X., Fan, L., Raychowdhury, R., Zeng, Q., et al. (2011). Full-length transcriptome assembly from RNA-Seq data without a reference genome. Nat. Biotechnol. *29*, 644–652.
39. Marlow, H., Tosches, M.A., Tomer, R., Steinmetz, P.R., Lauri, A., Larsson, T., and Arendt, D. (2014). Larval body patterning and apical organs are conserved in animal evolution. BMC Biol. *12*, 7.
40. Tosches, M.A., Bucher, D., Vopalensky, P., and Arendt, D. (2014). Melatonin signaling controls circadian swimming behavior in marine zooplankton. Cell *159*, 46–57.
41. Guindon, S., Dufayard, J.-F., Lefort, V., Anisimova, M., Hordijk, W., and Gascuel, O. (2010). New algorithms and methods to estimate maximum-likelihood phylogenies: assessing the performance of PhyML 3.0. Syst. Biol. *59*, 307–321.
42. Ronquist, F., Teslenko, M., van der Mark, P., Ayres, D.L., Darling, A., Höhna, S., Larget, B., Liu, L., Suchard, M.A., and Huelsenbeck, J.P. (2012). MrBayes 3.2: efficient Bayesian phylogenetic inference and model choice across a large model space. Syst. Biol. *61*, 539–542.